Carbohydrate Polymers 86 (2011) 956–961

Contents lists available at ScienceDirect

Carbohydrate Polymers

journal homepage: www.elsevier.com/locate/carbpol

Green synthesis of silver nanoparticles by chemical reduction with hyaluronan

Nianxin Xia, Yurong Cai, Tian Jiang, Juming Yao *

The Key Laboratory of Advanced Textile Materials and Manufacturing Technology of Ministry of Education, College of Materials and Textile, Zhejiang Sci-Tech University, Xiasha Higher Education Park, Hangzhou 310018, China

ARTICLE INFO

Article history:
Received 29 July 2010
Accepted 25 May 2011
Available online 1 June 2011

Keywords:
Hyaluronan
Silver nanoparticles
Reaction conditions
Surface enhanced Raman scattering (SERS)

ABSTRACT

The paper reported a facile and green synthesis of silver nanoparticles by using hyaluronan (HA) as a reducing agent and soft template. The effect of reaction conditions on the Ag nanoparticle formation was investigated using UV–vis spectrophotometer, field-emission scanning electron microscopy, transmission electron microscopy and X-ray diffraction. The application of Ag nanoparticles in surface enhanced Raman scattering (SERS) of HA was also evaluated. The results showed that the high pH value, temperature and molar ratio of HA to $AgNO_3$ could accelerate the reduction rate of Ag^+ and affect the Ag nanoparticle size. The Ag nanoplates could be fabricated with a low molar ratio of HA to $AgNO_3$ by aging, which may be due to the selective adsorption and desorption of HA on the different crystallographic planes of Ag nanoparticles. The enhancement of Raman scattering effect was greatly dependent on the size and morphology of Ag nanoparticles.

1. Introduction

Nanostructured noble metal materials have wide-ranging implications in the fields of photonics (You, Chompoosor, & Rotello, 2007), catalysis (Steffan, Jakob, Claus, & Lang, 2009), microelectronics (Sun, Yin, Mayers, Herricks, & Xia, 2002), biosensing (Chen et al., 2007) and antimicrobial functionalities (Du, Niu, Xu, Xu, & Fan, 2009), etc. Among these, the use of nanosized silver (Ag) particles as a substrate for enhancing the surface plasmon resonance has been widely reported (Nogueira, Soares-Santos, Cruz, & Trindade, 2002), in which the well-defined shape and structure of Ag nanoparticles are critical to the optimum enhancement. In the past decades, many effective methods have been developed for the synthesis of Ag nanoparticles (Hideki, Kanda, Shibata, Ohkubo, & Abe, 2006; Pastoriza-Santos & Liz-Marzaĭn, 2002; Sun & Xia, 2002; Van Hyning, Klemperer, & Zukoski, 2001). However, the environmental and biological risks are usually caused due to the use of noxious reducing and/or stabilizing agents in the synthesis procedures, like sodium borohydride (Van Hyning et al., 2001), hydrazine (Hideki et al., 2006) and N,N-dimethylformamide (Pastoriza-Santos & Liz-Marzaĭn, 2002), etc. With the increasing awareness of environmental protection, people are inclined to focus on the 'green chemistry'. For this purpose, the natural compounds like β-D-glucose (Raveendran, Fu, & Wallen, 2003) and chitosan (Wan, Sun, Li, & Li, 2004) were used to stabilize the Ag nanoparticles with other reducing agents. In addition, the soluble starch has been used as both the reducing and stabilizing agents to synthesize the Ag nanospheres via a one-pot 'green' method (Vigneshwaran, Nachane, Balasubramanya, & Varadarajan, 2006).

Hyaluronan (HA) is a natural polymer of repeated disaccharides, themselves composed of D-glucuronic acid and D-N-acetylglucosamine, linked together via alternating β-1,4 and β-1,3 glycosidic bonds. HA is distributed widely throughout connective, epithelial, and neural tissues. As one of the chief components of the extracellular matrix, hyaluronan contributes significantly to the cell proliferation and migration (Lapcik, Lapcik, De Smedt, Demeester, & Chabrecek, 1998). In this work, we used HA as the reducing agent to synthesize the Ag nanoparticles, in which the effect of reaction conditions, including the pH value, temperature, time and molar ratio of HA to $AgNO_3$ on the size and morphology of Ag nanoparticles was discussed. Furthermore, the surface enhanced Raman scattering (SERS) property of obtained Ag nanoparticles was investigated.

2. Experimental procedures

HA (molecular weight, 33 kDa) was purchased from Liuzhou Chemical Industry Group Co. Ltd. (China). Silver nitrate ($AgNO_3$) was purchase from Strem Chemicals, Inc. (USA). All other chemical reagents were purchased from Hangzhou Mike Chemical Agents Co. Ltd. (China), and were of analytical grade. Deionized water (18 MΩ cm) was used in the following experiments.

A total of 2 mL of $AgNO_3$ solution (50 mM) was added into 18 mL of HA solution (5 mM) in a 50 mL one-neck flask, in which the molar ratio of HA to $AgNO_3$ in the reaction system was kept as 1:1. After regulated the pH value by 1 M NaOH or 1 M HNO_3, the

* Corresponding author. Tel.: +86 571 86843618; fax: +86 571 86843619.
E-mail address: yaoj@zstu.edu.cn (J. Yao).

0144-8617/$ – see front matter © 2011 Elsevier Ltd. All rights reserved.
doi:10.1016/j.carbpol.2011.05.053

flask was capped and the mixture was stirred in the dark for different times at varied temperatures to obtain the yellowish colloidal samples.

To investigate the effect of HA content in the reaction system, a total of 2 mL of $AgNO_3$ solution (50 mM) was added into 18 mL of HA solution with varied concentrations (5 mM, 2.5 mM, 1 mM, 0.5 mM and 0.25 mM, respectively) in a 50 mL one-neck flask, in which the molar ratio of HA to $AgNO_3$ in the reaction system was varied from 1:1, 0.5:1, 0.2:1, 0.1:1 to 0.05:1. After reacted with stirring in dark at 70 °C and pH 11 for 2 h, the colloidal samples were transferred into an autoclave for aging at 70 °C for another 48 h. The above samples with varied HA contents were abbreviated as 1HA, 0.5HA, 0.2HA, 0.1HA and 0.05HA, respectively, according to the HA content in order.

All colloidal samples were characterized by a Perkin Elmer Lambda 900 UV–vis spectrophotometer from 200 to 800 nm with a scan rate of 300 nm/min. The Ag nanoparticles were collected from the colloidal solutions by centrifugation, washed with distilled water for three times, and dried at 40 °C for 24 h in vacuum. The XRD patterns were characterized with Thermo ARL X'TRA X-ray diffractometer using a monochromatic CuK_α radiation at $\lambda = 1.54056$ Å in the range of $2\theta = 35–90°$ with a scanning rate of 5.0°/min and a step size of 0.04°. For TEM and FE-SEM observation, the Ag nanoparticles were dispersed in distilled water under ultrasonic treatment, which were then dropped onto the carbon-coated copper grids for TEM observation using a JEOL 1230 transmission electron microscopy at 120 kV, and dropped onto the silicon wafers for FE-SEM using a JEOL S4800 field-emission scanning electron microscope at an acceleration voltage of 1 kV. For SERS analysis, 10 μL of the colloidal solution was dropped onto a glass slide followed by drying at 25 °C. The SERS spectra were recorded using a LabRAM HR-UV 800 micro-Raman spectroscopy using a laser beam with an excitation wavelength of 785 nm and a Peltier-cooled CCD detector at a power of 17 mW.

3. Results and discussion

3.1. Effect of reaction conditions on the Ag^+ reduction

Fig. 1a shows the effect of reaction temperature on the Ag^+ reduction by UV–vis spectroscopy, in which the experiments were performed under the conditions of pH 11 and 1:1 of HA to $AgNO_3$ (molar ratio). It is known that an absorption band appears at about 400–420 nm because of the surface plasmon resonance in Ag nanoparticles (Pastoriza-Santos & Liz-Marzaĭn, 1999; Pastoriza-Santos, Serra-Rodrıĭguez, & Liz-Marzaĭn, 2000). Here, no band in this region was observed on the UV–vis absorption spectrum of sample reacted at 25 °C even for 24 h. At both 50 °C and 70 °C, the golden yellow solutions were obtained accompanied with the appearance of absorption band at about 408 nm on the UV–vis spectra, suggesting the formation of nano-Ag colloids in these two systems. Also a temperature-dependent increase of peak intensity was observed, i.e., the spectrum for the sample reacted at 70 °C for 1 h had the extremely higher intensity at about 408 nm than that reacted at 50 °C for 8 h. So that, the Ag^+ reduction strongly relies on the reaction temperature, and the higher reaction temperature causes a higher reduction rate of Ag^+ (Pastoriza-Santos & Liz-Marzaĭn, 1999).

pH value is usually another key factor to the Ag^+ reduction. When the pH value is near to its isoelectric point (about 2.9 (Surini, Akiyama, Morishita, Nagai, & Takayama, 2003)), HA possesses uncharged carboxyl groups leading the molecular chains shrunk to a coiled state. When the pH value is higher than 2.9, the carboxyl groups will be negatively charged due to its hydrolysis, which makes the HA chains to be the linear conformation. So that, higher pH value of HA solution would lead to more exposed carboxyl groups electrostatically interacting with Ag^+, and promote the reduction rate of Ag^+ by HA (Cui et al., 2008). Fig. 1b shows the effect of reaction pH value on the Ag^+ reduction by UV–vis spectroscopy, in which the experiments were performed at 70 °C and 1:1 of HA to $AgNO_3$ (molar ratio). At pH 3.0, only a band at about 270 nm was observed even after 24 h of reaction, which cor-

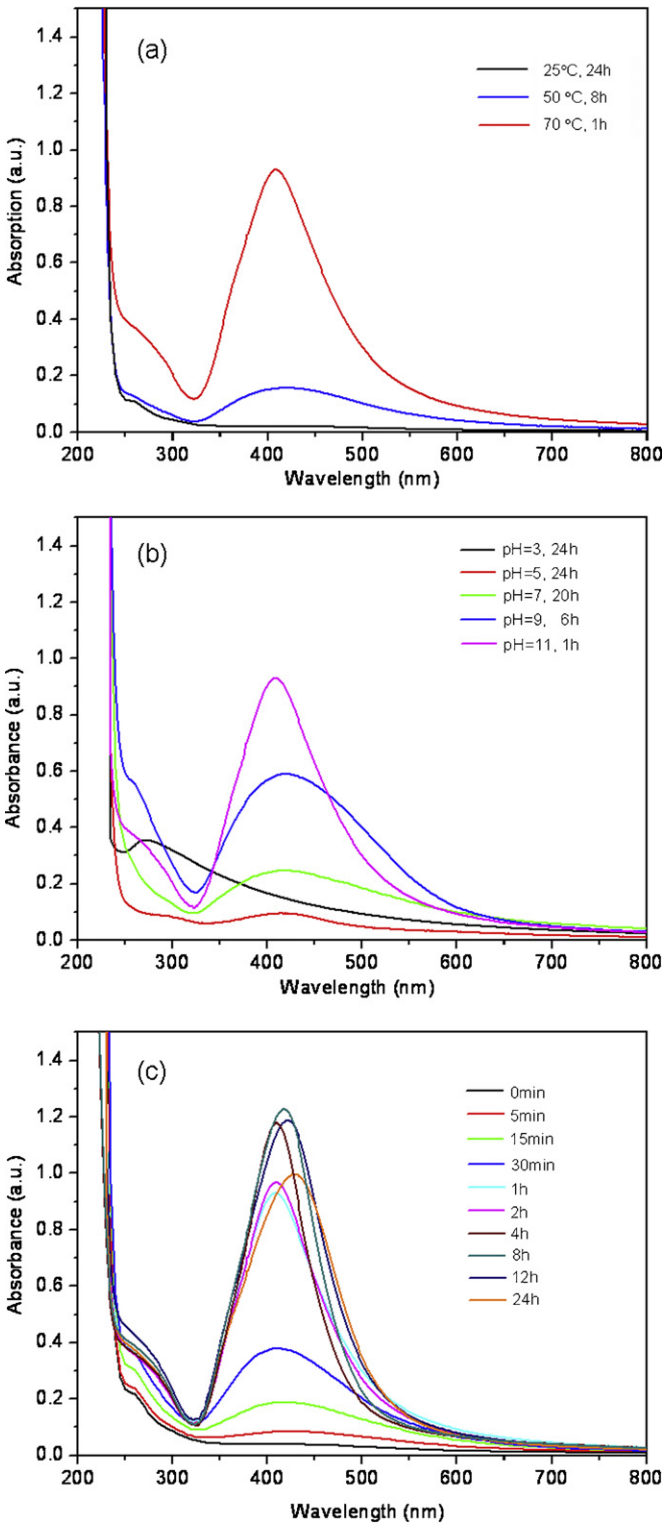

Fig. 1. (a) Temperature-dependent, (b) pH-dependent and (c) time-dependent UV–vis spectra of mixture solutions reacted with 1:1 of HA to $AgNO_3$ (molar ratio).

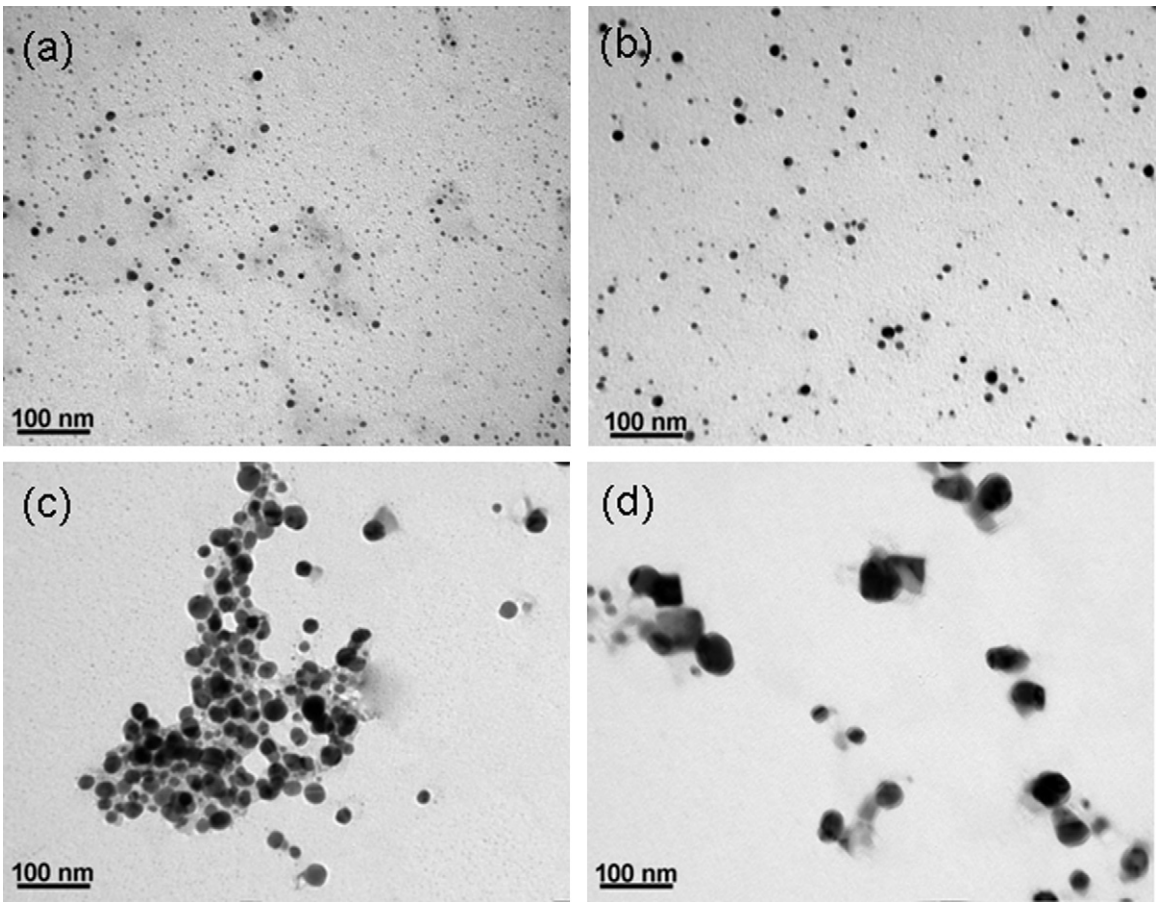

Fig. 2. TEM images of Ag nanoparticles synthesized at 70 °C and pH 11 with 1:1 of HA to $AgNO_3$ (molar ratio). The reaction time was (a) 1 h, (b) 4 h, (c) 8 h and (d) 24 h, respectively.

responded to the existence of Ag^+ clusters. With the increase of pH value, a new band appeared at about 408–422 nm on the UV–vis spectra of samples, suggesting the formation of Ag nanoparticles. Moreover, higher pH value led to the higher reduction rate of Ag^+. Table 1 summarized the maximum absorption wavelength (λ_{max}) corresponding to the Ag nanoparticles and their absorption peak intensity on the UV–vis spectra of samples reacted under different pH values. It could be found that both the λ_{max} and the absorption peak intensity increased gradually with the increase of pH value except the λ_{max} at pH 11 for 1 h. The amount and size of Ag nanoparticles are positively related with the adsorption peak intensity and the λ_{max} on the UV–vis spectra (Jradi et al., 2010; Wei et al., 2007), respectively. So that, when the reaction was carried out at a higher pH value, the Ag^+ could be reduced quickly to Ag particles, and the additional reaction time would promote the crystal growth of Ag particles leading to the higher λ_{max} and absorption peak inten-

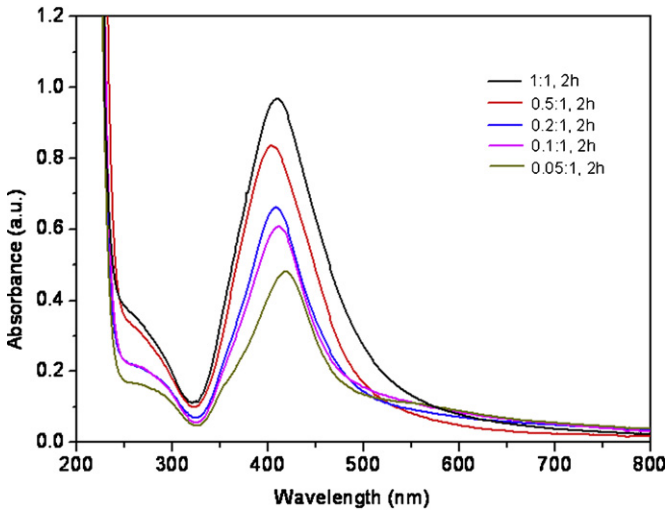

Fig. 3. UV–vis spectra of mixture solutions reacted for 2 h with different molar ratios of HA to $AgNO_3$ (molar ratio) at 70 °C and pH 11.

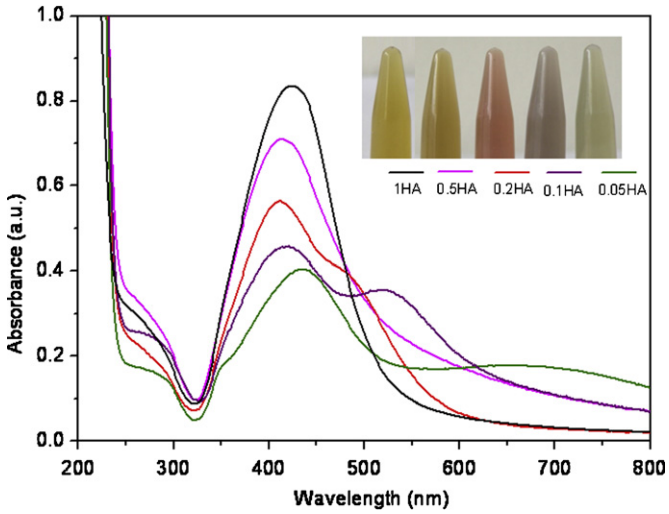

Fig. 4. UV–vis spectra of mixture solutions aged at 70 °C for 48 h after 2 h of reaction. Insert is the photo of solutions after aging.

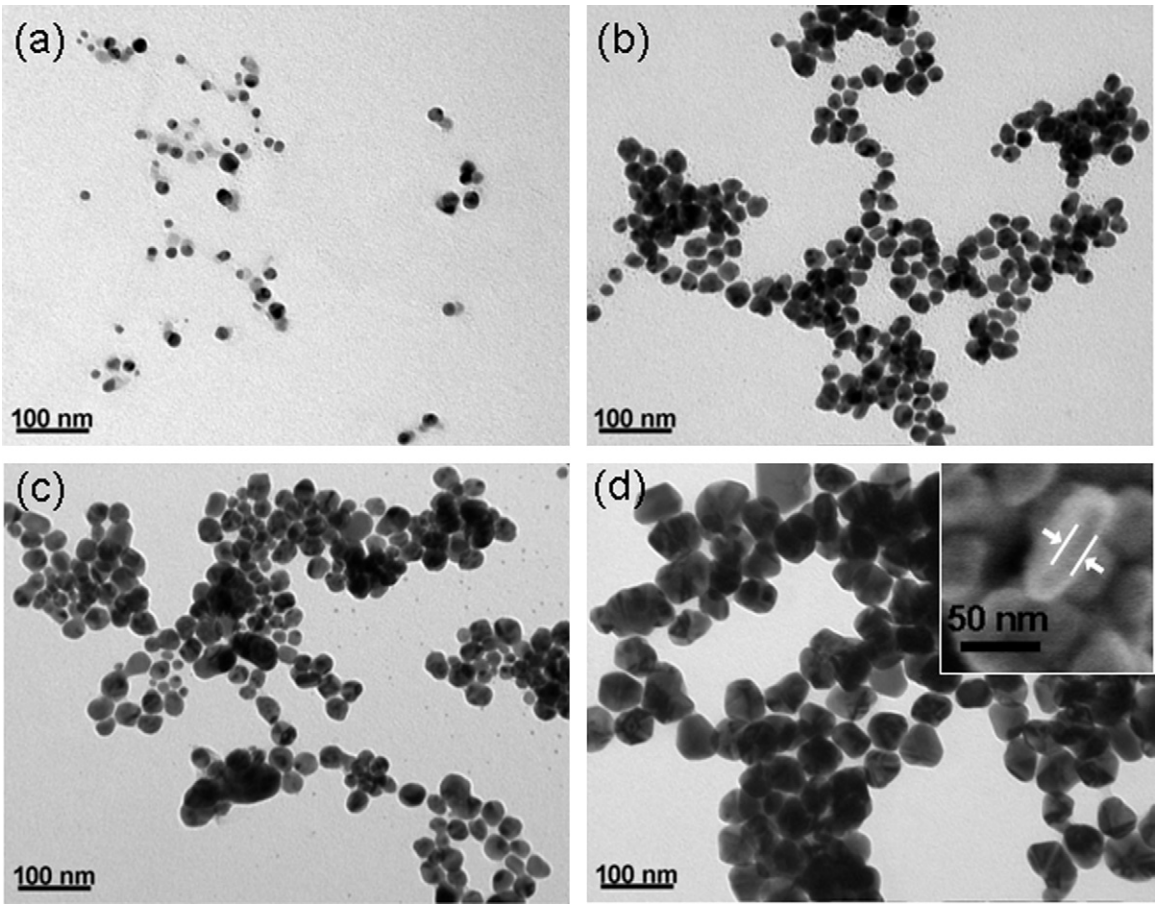

Fig. 5. TEM images of (a) 0.5HA, (b) 0.2HA, (c) 0.1HA and (d) 0.05HA. Insert in (d) is the FE-SEM image of 0.05HA.

sity. Here, the low λ_{max} at pH 11 for 1 h should be due to the short reaction time, which could be verified from Fig. 1c.

Fig. 1c shows the effect of reaction time on the Ag^+ reduction by UV–vis spectroscopy, in which the experiments were performed at 70 °C, pH 11 and 1:1 of HA to $AgNO_3$ (molar ratio). After 5 min of reaction, a slight absorption band at around 410 nm appeared, which became a clearly visible peak after 30 min, suggesting the presence of spherical Ag nanoparticles. The absorption peak intensity increased rapidly with the increase of reaction time to 4 h due to the continuous formation of Ag nanoparticles in the system (Jradi et al., 2010). However, further increase of reaction time from 4 h to 8 h did not increase the absorption peak intensity significantly but a red-shift appeared from 408 nm for 4 h to 418 nm for 8 h due to the increase of Ag nanoparticle size (Wei et al., 2007). A red shift occurred continuously from 418 nm to 429 nm when the reaction time increased from 8 h to 24 h, however the absorption peak intensity decreased alternatively, suggesting a period of predominant crystal growth of Ag nanoparticles in the reaction system by the assemble and amalgamation of small particles. The morphological change of Ag nanoparticles with the reaction time was further proved by TEM (Fig. 2). The average size of spherical Ag nanoparticles became larger and larger, which was about 7 nm, 15 nm, 30 nm and 40 nm corresponding to 1 h, 4 h, 8 h and 24 h of reaction times, respectively.

Table 1
Characteristics of Ag^+ reduction rate with respect to pH of aqueous solution.

pH value, Time (h)	λ_{max} (nm)	Absorption intensity
3, 24	/	/
5, 24	415	0.0945
7, 20	420	0.3298
9, 6	422	0.5891
11, 1	408	0.9307

3.2. Effect of HA content on the Ag^+ reduction

The HA content in the reaction system could also affect the reduction rate of Ag^+. Fig. 3 showed the effect of HA content on the Ag^+ reduction by UV–vis spectroscopy while keeping the $AgNO_3$ content unchanged, in which the experiments were performed at 70 °C and pH 11 for 2 h. Compared with that reacted with 1:1 of HA to $AgNO_3$ (molar ratio), longer reaction time was necessary when the HA content was decreased in the reaction system. For the same reaction time, the absorption peak intensity declined with the decrease of HA to $AgNO_3$ molar ratio from 1:1 to 0.05:1, accompanied with a slight red shift. Although the yellowish colloidal solutions from five reaction systems were similar to each other when the molar ratio decreased, the absorption peak intensity decreased from 0.56 to 0.48 and the corresponding λ_{max} shifted from 402 nm to 418 nm. This may be due to the fact that with the decrease of HA content, fewer Ag^+ was reduced and few HA molecules absorbed on the pre-formed particles resulting in the formation of large Ag clusters (Huang & Yang, 2004a; Huang & Yang, 2004b).

3.3. Synthesis of Ag nanoplates

The Ag nanoparticles obtained with different molar ratio of HA to $AgNO_3$ was further aged at 70 °C for another 48 h. Inter-

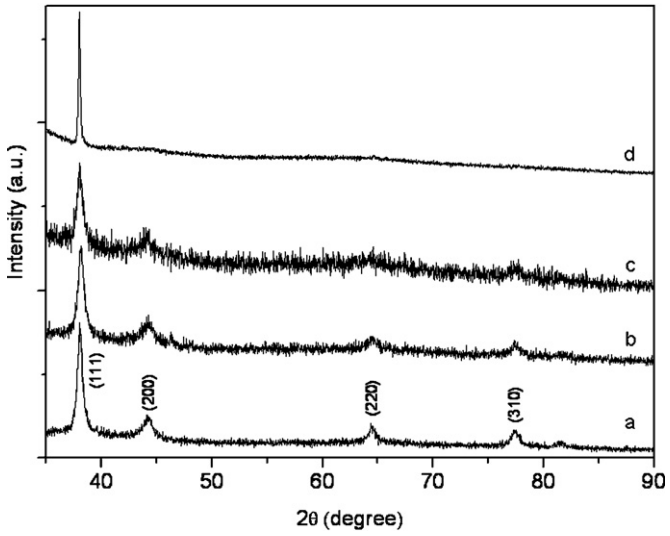

Fig. 6. XRD patterns of (a) 0.5HA, (b) 0.2HA, (c) 0.1HA and (d) 0.05HA.

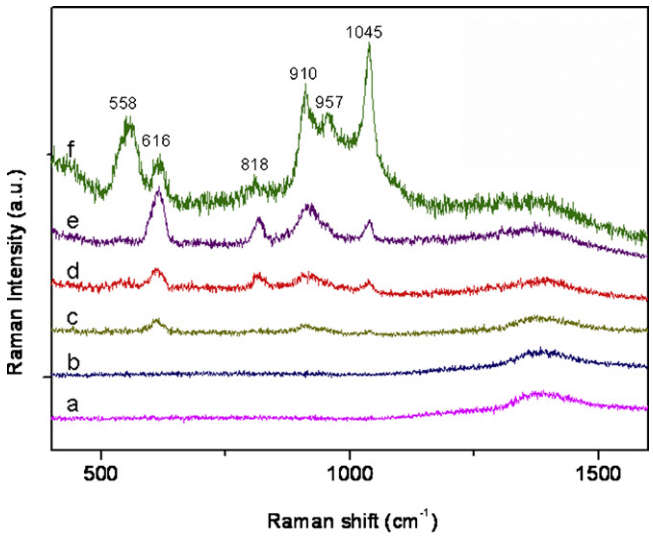

Fig. 7. SERS spectra of (a) glass substrate, (b) pure HA, (c) 0.5HA, (d) 0.2HA, (e) 0.1HA and (f) 0.05HA.

estingly, the colloidal solutions showed a color change from light yellow corresponding to 1:1 of HA to $AgNO_3$ to deep yellow, pink, purple, and green corresponding to 0.5:1, 0.2:1, 0.1:1 and 0.05:1, respectively (Fig. 4). The UV–vis spectra of 1HA and 0.5HA showed a sharp peak only at around 415 nm, indicating the presence of spherical Ag nanoparticles, which had an average size of <20 nm according to the TEM image in Fig. 5a. With the decrease of molar ratio of HA to $AgNO_3$ to 0.2:1, a shoulder was observed at around 480 nm on the UV–vis spectrum. When the molar ratio was 0.1:1, the sharp peak was at around 415 nm but its shoulder was red-shifted to about 522 nm due to the increased Ag nanoparticle size as shown in Fig. 5b and c. When the molar ratio was 0.05:1, the UV–vis spectrum exhibited a significantly red-shifted peak at 437 nm and a broad shoulder between 550 nm and 800 nm. The TEM image (Fig. 5d) showed that the sample became the truncated triangular nanoplates with around 35 nm in edge length and 15 nm in thickness. It was believed that the morphological change of Ag nanoparticles induced the discrepancy of UV–vis adsorption spectra in Fig. 4 (Gueĭvel et al., 2009).

To investigate the crystal structure of Ag nanoparticles after aging, the samples were further analyzed by XRD (Fig. 6). The XRD pattern of 0.5HA (Fig. 6a) clearly showed that there were four diffraction peaks, which could be attributed to (1 1 1), (2 0 0), (2 2 0) and (3 1 1) crystallographic planes of Ag nanoparticles, respectively. But the peaks for (2 0 0), (2 2 0) and (3 1 1) planes disappeared gradually when the molar ratio of HA to $AgNO_3$ decreased. Finally, only one diffraction peak indexed as (1 1 1) plane was left when the molar ratio was 0.05:1 due to the formation of Ag nanoplates which had the exclusive crystallographic plane of (1 1 1). The formation of Ag nanoparticles with different morphologies derived from varied HA content has not fully understood yet. However, during the first chemical reduction process, the Ag particles were formed in a fresh and homogeneous precursor solution and were covered uniformly by HA molecules, which led to the formation of spherical structure due to the uniformly growth of crystals (Maillard, Huang, & Brus, 2003; Wiley et al., 2005a; Wiley, Sun, Mayers, & Xia, 2005b). In the aging process, the adsorption and desorption of HA molecules on the different crystallographic planes of Ag nanoparticles were different, possibly leading to the eventual development of a non-spherical geometry (Sun et al., 2002).

3.4. SERS properties

It is well-known that the nano-Ag materials with certain size and morphology exhibit the SERS properties. The SERS spectra of Ag nanoparticles synthesized with varied HA contents after aging were shown in Fig. 7, where no signal was detected for the HA alone on the glass substrate. As expected, the Ag nanoparticles synthesized with HA exhibited some signals on their SERS spectra, in which the SERS enhancement was greatly dependent on the size and shape of nano-Ag materials. Compared with the SERS spectrum of 0.5HA with smaller particle size, the spectra of 0.2HA and 0.1HA had stronger signals, suggesting that larger Ag nanoparticles had the strong SERS enhancement for HA. Moreover, the Ag nanoplates of 0.05HA displayed more signals than the Ag spherical nanoparticles at 957 cm^{-1} and 1045 cm^{-1}, which corresponded to the skeletal vibrations associated with the β linkages, and C–C and C–O stretching, respectively (Alkrad, Mrestani, Stroehl, Wartewig, & Neubert, 2003; Reineck, DeAnna, Suleski, Lee, & Rupprecht, 2003). The enhancement efficiency at 1045 cm^{-1} from the Ag nanoplates was about dozens of times higher than that from the Ag spherical nanoparticles, which could be ascribed to the localized surface plasmon resonance adsorption of nanoplates in the near infrared region (Lu, Kobayashi, Tawa, & Ozaki, 2006; Zhang, Li, Sun, & Li, 2005).

4. Conclusion

A facile, green way was reported for the synthesis of Ag nanostructure materials using HA as the reducing agent and soft template. It was found that the high pH value, temperature and molar ratio of HA to $AgNO_3$ could accelerate the reduction rate of Ag^+ and affect the Ag nanoparticle size. The Ag nanoplates were fabricated with a low molar ratio of HA to $AgNO_3$ by aging, which could be ascribed to the selective adsorption and desorption of HA on the different crystallographic planes of Ag nanoparticles. The obtained Ag nanomaterials with different sizes and morphologies showed the different enhancement for the surface Raman scattering signals of HA, among which the Ag nanoplate possessed the strongest effect. The work may provide a potential application of Ag nanostructure materials in the field of SERS and biosensing.

Acknowledgements

The work is financially supported by the Program for New Century Excellent Talents in University (NCET070763) and Zhejiang Natural Science Foundation of China (Y4090416).

References

Alkrad, J. A., Mrestani, Y., Stroehl, D., Wartewig, S., & Neubert, R. (2003). Characterization of enzymatically digested hyaluronic acid using NMR, Raman, IR, and UV–vis spectroscopies. *Journal of Pharmaceutical and Biomedical Analysis*, *31*, 545–550.

Chen, J. Y, Wang, D. L., Xi, J. F., Au, L., Siekkinen, A., Warsen, A., et al. (2007). Immuno gold nanocages with tailored optical oroperties for targeted photothermal destruction of cancer cells. *Nano Letters*, *7*, 1318–1322.

Cui, X. Q., Li, C. M., Bao, H. F., Zheng, X. T., Zang, J. F., Ooi, C. P., et al. (2008). Hyaluronan-assisted photoreduction synthesis of silver nanostructures: From nanoparticle to nanoplate. *Journal of Physical Chemistry C*, *112*, 10730–10734.

Du, W. L., Niu, S. S., Xu, Y. L., Xu, Z. R., & Fan, C. L. (2009). Antibacterial activity of chitosan tripolyphosphate nanoparticles loaded with various metal ions. *Carbohydrate Polymers*, *75*, 385–389.

Gueĭvel, X. L., Wang, F. Y., Stranik, O., Nooney, R., Gubala, V., McDonagh, C., et al. (2009). Synthesis, stabilization, and functionalization of silver nanoplates for biosensor applications. *Journal of Physical Chemistry C*, *113*, 16380–16386.

Hideki, S, Kanda, T., Shibata, H., Ohkubo, T., & Abe, M. (2006). Preparation of highly dispersed core/shell-type titania nanocapsules containing a single Ag nanoparticle. *Journal of the American Chemical Society*, *128*, 4944–4945.

Huang, H. Z., & Yang, X. R. (2004a). Synthesis of chitosan-stabilized gold nanoparticles in the absence/presence of tripolyphosphate. *Biomacromolecules*, *5*, 2340–2346.

Huang, H. Z., & Yang, X. R. (2004b). Synthesis of polysaccharide-stabilized gold and silver nanoparticles: A green method. *Carbohydrate Research*, *339*, 2627–2631.

Jradi, S., Balan, L., Zeng, X. H., Plain, J., Lougnot, D. J., Royer, P., et al. (2010). Spatially controlled synthesis of silver nanoparticles and nanowires by photosensitized reduction. *Nanotechnology*, *21*, 95605–95612.

Lapcik, L., Lapcik, L., De Smedt, S., Demeester, J., & Chabrecek, P. (1998). Hyaluronan: Preparation, structure, properties, and applications. *Chemical Reviews*, *98*, 2663–2684.

Lu, L. H., Kobayashi, A., Tawa, K., & Ozaki, Y. (2006). Silver nanoplates with special shapes: controlled synthesis and their surface plasmon resonance and surface-enhanced Raman scattering properties. *Chemistry of Materials*, *18*, 4894–4901.

Maillard, M., Huang, P. R., & Brus, L. (2003). Silver nanodisk growth by surface plasmon enhanced photoreduction of adsorbed [Ag^+]. *Nano Letters*, *3*, 1611–1615.

Nogueira, H. I., Soares-Santos, P. C., Cruz, S. M., & Trindade, T. (2002). Adsorption of 2, 2-dithiodipyridine as a tool for the assembly of silver nanoparticles. *Journal of Materials Chemistry*, *12*, 2339–2342.

Pastoriza-Santos, I., & Liz-Marzaĭn, L. M. (1999). Formation and stabilization of silver nanoparticles through reduction by N,N-dimethylformamide. *Langmuir*, *15*, 948–951.

Pastoriza-Santos, I., & Liz-Marzaĭn, L. M. (2002). Synthesis of silver nanoprisms in DMF. *Nano Letters*, *2*, 903–905.

Pastoriza-Santos, I., Serra-Rodriĭguez, C., & Liz-Marzaĭn, L. M. (2000). Self-assembly of silver particle monolayers on glass from Ag+ solutions in DMF. *Journal of Colloid and Interface Science*, *221*, 236–241.

Raveendran, P., Fu, J., & Wallen, S. L. (2003). Completely "green" synthesis and stabilization of metal nanoparticles. *Journal of the American Chemical Society*, *125*, 13940–13941.

Reineck, I., DeAnna, J., Suleski, T. J., Lee, S. A., & Rupprecht, A. (2003). A Raman study of the hydration of wet-spun films of Li-hyaluronate. *Journal of Biomolecular Structure and Dynamics*, *21*, 153–158.

Steffan, V. M., Jakob, A., Claus, P., & Lang, H. (2009). Silica supported silver nanoparticles from a silver(I) carboxylate: Highly active catalyst for regioselective hydrogenation. *Catalysis Communications*, *10*, 437–441.

Sun, Y., & Xia, Y. N. (2002). Shape-controlled synthesis of gold and silver nanoparticles. *Science*, *298*, 2176–2179.

Sun, Y., Yin, Y., Mayers, B. T., Herricks, T., & Xia, Y. N. (2002). Uniform silver nanowires synthesis by reducing $AgNO_3$ with ethylene glycol in the presence of seeds and poly(vinyl pyrrolidone). *Chemistry of Materials*, *14*, 4736–4745.

Surini, S., Akiyama, H., Morishita, M., Nagai, T., & Takayama, K. (2003). Release phenomena of insulin from an implantable device composed of a polyion complex of chitosan and sodium hyaluronate. *Journal of Controlled Release*, *90*, 291–301.

Van Hyning, D. L., Klemperer, W. G., & Zukoski, C. F. (2001). Characterization of colloidal stability during precipitation reactions. *Langmuir*, *17*, 3120–3127.

Vigneshwaran, N., Nachane, R. P., Balasubramanya, R. H., & Varadarajan, P. V. (2006). A novel one-pot 'green' synthesis of stable silver nanoparticles using soluble starch. *Carbohydrate Research*, *341*, 2012–2018.

Wan, A., Sun, Y., Li, G., & Li, H. L. (2004). Preparation of aspirin and probucol in combination loaded chitosan nanoparticles and in vitro release study. *Carbohydrate Polymers*, *75*, 31–37.

Wei, G., Wang, L., Sun, L. L., Song, Y. H., Sun, Y. J., Guo, C. L., et al. (2007). Type I collagen-mediated synthesis and assembly of UV-photoreduced gold nanoparticles and their application in surface enhanced Raman scattering. *Journal of Physical Chemistry C*, *111*, 1976–1982.

Wiley, B., Sun, Y. G., Chen, J. Y., Cang, H., Li, Z. Y., Li, X. D., et al. (2005). Shape-controlled synthesis of silver and gold nanostructures. *MRS Bulletin*, *30*, 356–361.

Wiley, B., Sun, Y. G., Mayers, B., & Xia, Y. N. (2005). Shape-controlled synthesis of metal nanostructures: The case of silver. *Chemistry – A European Journal*, *11*, 454–463.

You, C. C., Chompoosor, A., & Rotello, V. M. (2007). The biomacromolecule-nanoparticle interface. *Nanotoday*, *2*, 34–43.

Zhang, J., Li, X. L., Sun, X. M., & Li, Y. D. (2005). Surface enhanced Raman scattering effects of silver colloids with different shapes. *Journal of Physical Chemistry B*, *109*, 12544–12548.